Available online at www.sciencedirect.com

ScienceDirect

Materials Today: Proceedings 5 (2018) 26495–26500

materialstoday: PROCEEDINGS

www.materialstoday.com/proceedings

DAS_2017

Experimental investigation of the shear angle variation during orthogonal cutting

Szabolcs Berezvai[a,*], Tamas G. Molnar[a], Daniel Bachrathy[a], Gabor Stepan[a]

[a]*Budapest University of Technology and Economics, Faculty of Mechanical Engineering, Department of Applied Mechanics, Műegyetem rkp. 5., Budapest H-1111, Hungary*

Abstract

In this paper, we investigate the variation of the shear angle during orthogonal cutting processes. In orthogonal cutting, the material in front of the cutting edge is sheared over a primary shear zone that is approximated by the shear plane. The so-called shear angle corresponding to the shear plane has significant role in theoretical cutting force models and in the dynamics of cutting. This paper is dedicated to determining the shear angle experimentally for stationary and non-stationary cutting based on high-speed camera recordings and cutting force measurements. Furthermore, the relationship between simple theoretical shear angle models and the measured shear angle variation is also provided.

Selection and/or Peer-review under responsibility of the Committee Members of 34th DANUBIA ADRIA SYMPOSIUM on Advances in Experimental Mechanics (DAS 2017).

Keywords: Metal cutting; Machine tool vibration; Chip formation; Shear plane; High-speed camera;

1. Introduction

The performance of metal cutting processes are often limited by the occurrence of harmful self-excited vibrations called machine tool chatter. Chatter is typically hard-to-predict and it has several undesired consequences: it produces unpleasant noise, leads to poor surface quality, limits the achievable productivity, increases tool wear, and it may even damage the workpiece or the tool. Hence, there is significant need to understand the dynamics of the

* Corresponding author. Szabolcs Berezvai. Tel.: +36-1-463-1332; fax: +36-1-463-1369.
E-mail address: berezvai@mm.bme.hu

Selection and/or Peer-review under responsibility of the Committee Members of 34th DANUBIA ADRIA SYMPOSIUM on Advances in Experimental Mechanics (DAS 2017).

chip formation process during machining. In the typical mechanical models of metal cutting, self-excited vibrations in the workpiece–machine-tool system are explained by the so-called regenerative effect [1-4]. These models rely on theoretical cutting force expressions, which are affected by several cutting parameters including shear angle, friction coefficient and tool geometry [5,6]. Consequently, modelling and measuring the shear angle is important in terms of developing accurate cutting force expressions to investigate the dynamics of metal cutting processes.

The simplest machining operation, where the chip formation process and the shear layer can be investigated, is orthogonal cutting, which can be exactly realized by planing processes, only. In orthogonal cutting, the material in front of the cutting edge is sheared over a zone that is approximated by the shear plane located at shear angle Φ [5,6]. The shear angle determines the magnitude and direction of the cutting force acting on the tool. In the literature, theoretical shear angle models can be found to describe stationary cutting processes, where the uncut chip thickness is constant in time. However, the uncut chip thickness may vary in time during cutting, especially in the case of machine tool vibrations in turning, or even in idealized vibration free milling processes.

The goal of this contribution is to determine the shear angle experimentally during stationary and non-stationary orthogonal cutting and to compare the results with the prediction of theoretical models. Since, the time-scale of the chip formation is in the range of microseconds for a typical metal cutting process, a possible solution to observe such phenomena is to use high-speed camera system and to determine the shear angle based on image detection algorithms.

The outline of the paper is the following: In Section 2, theoretical shear angle models are summarized. The details and results of experimental cutting tests are provided in Section 3, while Section 4 discusses the shear angle detection algorithm. The comparison of the theoretical models and the experimental results are presented in Section 5. The results of the paper are summarized in Section 6.

2. Shear angle models

In the mechanical model of orthogonal cutting, there are three deformation zones that are presented in Figure 1. Initially, the material in front of the tool is sheared over the primary zone and this forms the chip. The chip undergoes further deformation as it slides along the rake face of the tool, which is called the secondary zone, while the friction area between the flank of the tool and the freshly machined surface is the tertiary zone. According to the assumption of Merchant, the shear zone is a plane. By definition, the shear angle Φ is the angle between the cutting speed v_c and the shear plane [4,5].

The most well-known approach of modelling cutting forces of stationary cutting processes is Merchant's circle [4,5] illustrated in Figure 1/b, where the uncut chip thickness h is assumed to be constant. In this model, the cutting force component $\mathbf{F}_S$ aligned with the shear plane is calculated as the product of the yield shear stress and the shear plane area $\left(\mathbf{F}_S = A_S \boldsymbol{\tau}_S\right)$. Consequently, the other components $\left(\mathbf{F}_\mathrm{n}, \mathbf{F}_\mathrm{u}, \mathbf{F}_\mathrm{v}, \mathbf{F}_\mathrm{f}, \mathbf{F}_\mathrm{t}\right)$ of the cutting force $\mathbf{F}$ can also be determined based on the rake angle α_r and the average friction angle β_a.

In the literature, the most commonly applied shear angle models are based on the maximum shear stress principle (MSSP) and the minimum energy principle (MEP) [5]. In both cases the shear stress $\boldsymbol{\tau}_S$ is assumed to be equivalent to the yield shear stress of the material, while the material of the workpiece is perfectly rigid-plastic.

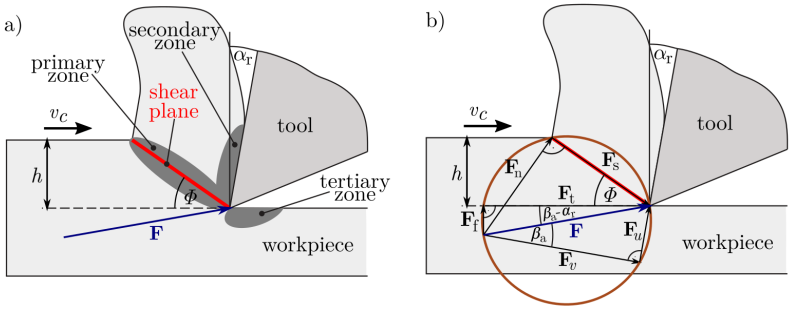

Fig. 1. (a) The deformation zones and shear plane; (b) Merchant's model of cutting forces

2.1. Maximum shear stress principle

According to MSSP, the shear occurs in the direction of maximum shear stress. This yields that the angle between the cutting force acting on the tool and the maximum shear stress must be $\pi/4$. Thus, based on Figure 1, the shear angle can be expressed as [5]

$$\Phi^{MSSP} = \frac{\pi}{4} - \left(\beta_a - \alpha_r\right). \tag{1}$$

2.2. Minimum energy principle

Let us introduce the power of the cutting force as $P = F_t v_c$, where F_t is the magnitude of the tangential cutting force component (see Figure 1/b). The MEP assumes that the power of the cutting force is minimal, letting $\mathrm{d}P/\mathrm{d}\Phi = 0$. Therefore, the shear angle can be determined accordingly as [5]

$$\Phi^{MEP} = \frac{\pi}{4} - \frac{\beta_a - \alpha_r}{2}. \tag{2}$$

Note, that in both cases, the shear angle depends only on α_r and β_a, thus the shear angle can be determined experimentally from measured cutting force signals and the tool geometry. Additionally, it can be seen that the MEP predicts larger shear angle than the MSSP, namely $\Phi^{MEP} > \Phi^{MSSP}$.

3. Experimental layout and results

The performance of the shear angle models has been investigated experimentally during orthogonal planing of a single aluminum (A2024-T351) rib of thickness $w = 2$ mm using the feed motion of a NCT EmR-610Ms CNC milling machine; the workpiece was moving in the *x*-direction and the tool in *z*-direction. As the experimental setup shows (see Figure 2/a), the workpiece was placed on a Kistler 9129AA multicomponent dynamometer for measuring the cutting force components in the $(x\text{-}y\text{-}z)$ coordinate system. A carbide tool was used with rake angle α_r =15° and flank angle α_f=10°. The cutting speed v_c was set between 5,000 and 10,000 mm/min.

The orthogonal cutting tests were performed using stationary (S) and non-stationary (NS) prescribed chip thicknesses (toolpaths), which were defined as

$$h^S(x) = h_0^S \quad \text{and} \quad h^{NS}(x) = h_0^{NS} + h_A^{NS}\sin(2\pi x/\lambda + \delta), \tag{3}$$

where $x = v_c t$, while the applied parameters were $h_0^S = 0.1$ mm and $h_0^{NS} = 0.05$ mm, respectively. The non-stationary chip thickness variation was characterized by the amplitude $h_A^{NS} = 0.1$ mm and the wavelength $\lambda = 10$ mm. Note, that due to the uncertainties in the positioning of the workpiece, the exact phase shift value δ can be determined from the test results only.

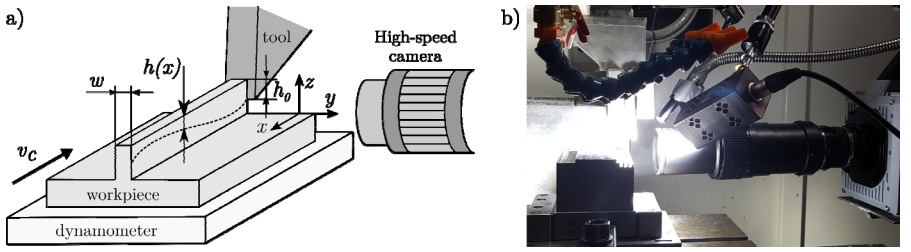

Fig. 2. (a) The schematics of the experimental setup; (b) the layout of the high-speed camera system during measurements

Additionally, the chip formation process was investigated via high-speed camera recordings using Photron SA5 high-speed camera system with 10,000 fps [7]. The layout of the high-speed camera system is presented in Figure 2/b. To ensure adequate magnification, the camera was equipped with Canon MP-E 65 mm macro lens, while the lighting was provided by Vision Device VD7000 LED (max. power 72W) and Hayashi HDF7010 Fiber Optic LED (max. power 155W) systems.

3.1. Variation of cutting forces

The variation of the measured cutting force components are presented in Figure 3. The spikes of the signals show that chip segmentation occurs during the non-stationary cutting test when the depth of cut is high enough. It can also be seen that the occurrence of segmentation (see the dark gray-shaded area in Figure 3/b) is not symmetric with respect to the peaks (dash-dot line in Figure 3/b) of sinusoidal chip thickness function $h^{NS}(x)$, which demonstrates significant hysteresis.

The angle $\beta_a - \alpha_r$ (see Figure 1) can be obtained from the measured cutting force components $\left(F_x, F_z\right)$ using $\beta_a - \alpha_r = \arctan(F_z / F_x)$, from which the theoretical shear angle approximations in Eqs. (1)-(2) can be evaluated.

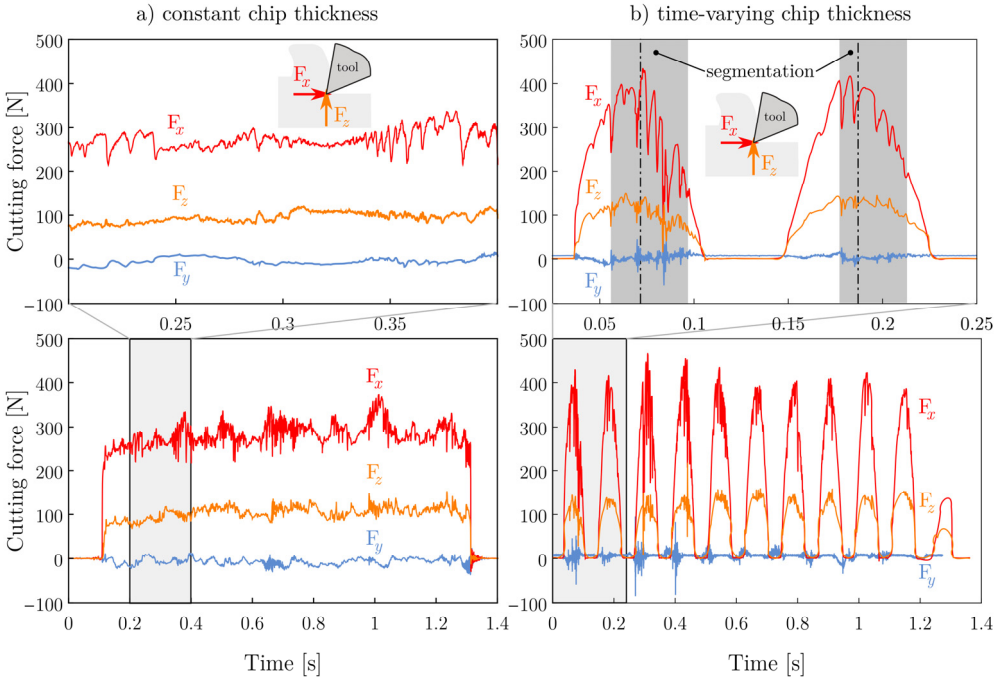

Fig. 3. The measured force signals in case of (a) stationary $\left(w = 2 \text{ mm};\ \alpha_r = 15°;\ \alpha_f = 10°;\ v_c = 10000 \text{ mm/min};\ h_0 = 0.1 \text{ mm}\right)$ and (b) non-stationary (sinusoidal) $\left(w = 2 \text{ mm};\ \alpha_r = 15°;\ \alpha_f = 10°;\ v_c = 5000 \text{ mm/min};\ h_0^{NS} = 0.05 \text{ mm};\ h_A^{NS} = 0.1 \text{ mm};\ \lambda = 10 \text{ mm}\right)$ chip thicknesses

4. Shear angle detection

The shear plane was detected using the following displacement-based image processing technique, which was applied on the high-speed camera recordings. The displacement values $\Delta\mathbf{r}_i = \left(\Delta x_i, \Delta z_i\right)$ were obtained for each material point of the workpiece from two subsequent video frames (see Figure 4). The occurrence of vertical displacement values (Δz_i) indicated the points that correspond to the shear plane. The shear plane was defined by fitting a straight line to these detected points in each frame, whereas the shear angle was calculated from the slope of the fitted lines. It should be emphasized, however, that the displacement field is typically very noisy, thus Wiener-filtering was applied before the evaluation of the displacement field.

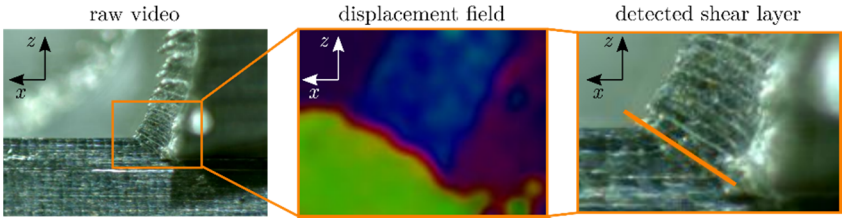

Fig. 4. The steps of the image processing algorithm

4.1. Correction of the non-stationary shear angle

As it was discussed in Section 2, the theoretical shear angle models assume that the uncut chip thickness is constant in time. The non-stationary chip thickness in Eq. (3), however, means that the vertical relative velocity v_z between the tool and the workpiece is nonzero. Using the non-stationary chip thickness $h^{NS}(x)$, the velocity v_z reads

$$v_z = \frac{\mathrm{d}h^{NS}(t)}{\mathrm{d}t} = \frac{\mathrm{d}h^{NS}(x)}{\mathrm{d}x}\frac{\mathrm{d}x}{\mathrm{d}t} = h_A \frac{2\pi}{\lambda} v_c \cos\left(\frac{2\pi}{\lambda} v_c t + \delta\right). \tag{4}$$

This yields, that the correction angle $\gamma = \arctan(v_z / v_c)$ should be introduced and added (see Figure 5/a) to the model-based shear angle values Φ using Eqs. (1)-(3). Thus, the corrected shear angle is calculated as

$$\Phi_{corr} = \Phi + \gamma. \tag{5}$$

Additionally, the phase shift δ should be known for the evaluation of the shear angle correction. It was determined by fitting the phase shift of the non-stationary chip thickness function $h^{NS}(x)$ to that of the tracked vertical tool position as shown by Figure 5/b. As a result of the fitting, the phase shift became $\delta = 0.0499$ rad.

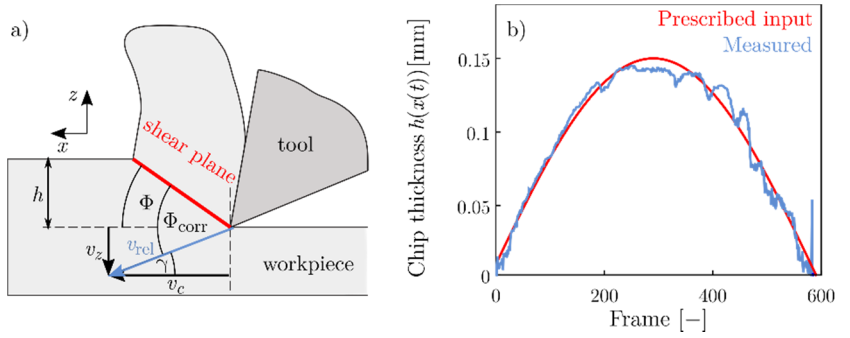

Fig. 5. (a) The direction of the relative velocity and its effect on the shear angle; (b) prescribed and measured non-stationary chip thickness

5. Results

The variation of the detected shear angle can be compared to the predictions of the theoretical models in Eqs. (1)-(2). Figure 6/a shows that between frames 0 and 162 (see dashed line), where built-up edge formation occurred, the MEP gives the better result. However, after the release of the built-up edge, the MSSP is gives better prediction. Figure 6/b is depicted for a single period of the non-stationary (sinusoidal) cutting tests, and it shows that the MEP gives a better approximation of the shear angle. However, at the beginning of sinusoidal toolpath, both the MSSP and MEP overestimated the shear angle, while during segmentation (in the gray shaded area of Figure 6/b) the qualitative predictions of both models are accurate.

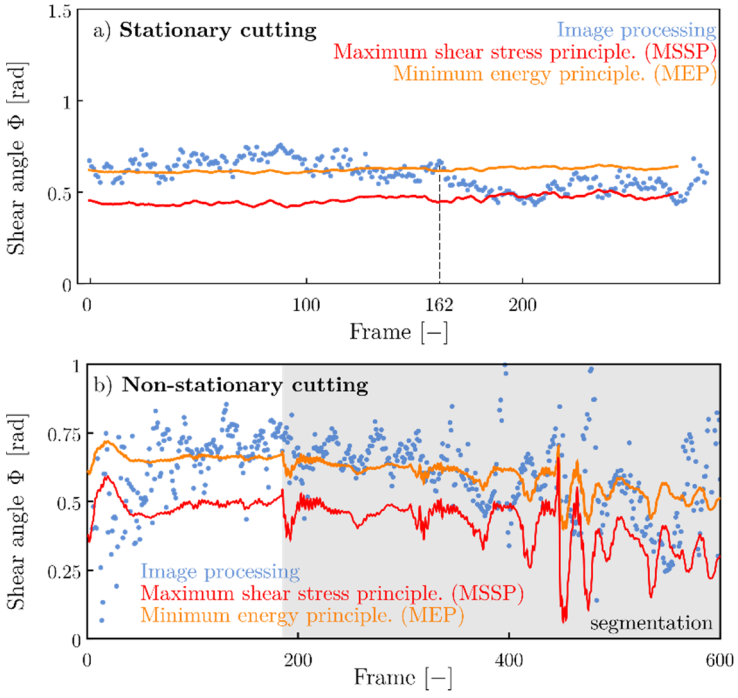

Fig. 6. Comparison of measured and theoretical shear angle values in case of (a) stationary and (b) non-stationary chip thicknesses

6. Conclusion

It can be concluded that the variation of the shear angle during orthogonal cutting can be measured using high-speed camera recordings and a displacement-based image detection algorithm. The cutting test revealed that the shear angle model based on the minimum energy principle gives better prediction for the shear angle variation in case of non-stationary cutting processes than the one based on the maximum shear stress principle. In addition, the shear angle is affected by chip segmentation, which typically occurs at high depths of cut. The occurrence of segmentation was found to exhibit significant hysteresis with respect to the variations of the chip thickness.

Acknowledgements

This research has been supported by the ÚNKP-17-3-I. New National Excellence Program of the Ministry of Human Capacities, Hungary. The research leading to these results has received funding from the European Research Council under the European Union's Seventh Framework Programme (FP/2007-2013) / ERC Advanced Grant Agreement n. 340889.

References

[1] S.A. Tobias, W. Fishwick, *Theory of regenerative machine tool chatter*, The Engineer. 205(7) (1958) 199-239
[2] J. Tlusty and M. Polacek, *The stability of the machine tool against self-excited vibration in machining.* ASME Prod. Eng. Res. Conf. Pittsburg. (1963), 454-465
[3] E. Budak, Y. Altintas, *Analytical Prediction of Chatter Stability in Milling – Part I*, J. Dyn. Sys., Meas., Control. 120 (1998) 22-30
[4] G. Stepan, *Retarded Dynamical Systems: Stability and Characteristic Functions,* Longman, Harlow, 1989
[5] Y. Altintas. *Manufacturing Automation – Metal Cutting Mechanics, Machine Tool Vibrations and CNC Design*, 2nd ed, Cambridge University Press, Cambridge, 2012
[6] M.E. Merchant. *Mechanics of the metal cutting process II: Plasticity conditions in orthogonal cutting.* J. Appl. Phys. 16 (1945) 318-324
[7] Y. Guo, W.D. Compton, S. Chandrasekar, *In situ analysis of flow dynamics and deformation fields in cutting and sliding of metals,* Proc. R. Soc. A. 471 (2015)